Gene Expression, Vol. 20, pp. 89–103
Printed in the USA.

1052-2166/20 $90.00 + .00
DOI: https://doi.org/10.3727/105221620X15889714507961
E-ISSN 1555-3884
www.cognizantcommunication.com

Downregulation of p16 Decreases Biliary Damage and Liver Fibrosis in the Mdr2$^{-/-}$ Mouse Model of Primary Sclerosing Cholangitis

Konstantina Kyritsi,* Heather Francis,*† Tianhao Zhou,‡ Ludovica Ceci,* Nan Wu,* Zhihong Yang,† Fanyin Meng,*† Lixian Chen,* Leonardo Baiocchi,§ Debjyoti Kundu,† Lindsey Kennedy,† Suthat Liangpunsakul,*† Chaodong Wu,¶ Shannon Glaser,‡ and Gianfranco Alpini*†

*Richard L. Roudebush VA Medical Center, Indianapolis, IN, USA
†Hepatology and Gastroenterology, Medicine, Indiana University, Indianapolis, IN, USA
‡Department of Medical Physiology, Texas A&M University College of Medicine, Bryan, TX, USA
§Liver Unit, Department of Medicine, University of Rome "Tor Vergata," Rome, Italy
¶Department of Nutrition, Texas A&M University, College Station, TX, USA

Biliary senescence and hepatic fibrosis are hallmarks of cholangiopathies including primary sclerosing cholangitis (PSC). Senescent cholangiocytes display senescence-associated secretory phenotypes [SASPs, e.g., transforming growth factor- 1 (TGF- 1)] that further increase biliary senescence (by an autocrine loop) and trigger liver fibrosis by paracrine mechanisms. The aim of this study was to determine the effect of p16 inhibition and role of the TGF- 1/microRNA (miR)-34a/sirtuin 1 (SIRT1) axis in biliary damage and liver fibrosis in the Mdr2$^{-/-}$ mouse model of PSC. We treated (i) in vivo male wild-type (WT) and Mdr2$^{-/-}$ mice with p16 Vivo-Morpholino or controls before measuring biliary mass [intrahepatic bile duct mass (IBDM)] and senescence, biliary SASP levels, and liver fibrosis, and (ii) in vitro intrahepatic murine cholangiocyte lines (IMCLs) with small interfering RNA against p16 before measuring the mRNA expression of proliferation, senescence, and fibrosis markers. p16 and miR-34a increased but SIRT1 decreased in Mdr2$^{-/-}$ mice and PSC human liver samples compared to controls. p16 immunoreactivity and biliary senescence and SASP levels increased in Mdr2$^{-/-}$ mice but decreased in Mdr2$^{-/-}$ mice treated with p16 Vivo-Morpholino. The increase in IBDM and hepatic fibrosis (observed in Mdr2$^{-/-}$ mice) returned to normal values in Mdr2$^{-/-}$ mice treated with p16 Vivo-Morpholino. TGF- 1 immunoreactivity and biliary SASPs levels were higher in Mdr2$^{-/-}$ compared to those of WT mice but returned to normal values in Mdr2$^{-/-}$ mice treated with p16 Vivo-Morpholino. The expression of fibrosis/senescence markers decreased in cholangiocytes from Mdr2$^{-/-}$ mice treated with p16 Vivo-Morpholino (compared to Mdr2$^{-/-}$ mice) and in IMCLs (after p16 silencing) compared to controls. Modulation of the TGF- 1/miR-34a/SIRT1 axis may be important in the management of PSC phenotypes.

Key words: Biliary epithelium; Cholangiocytes; Cholangiopathies; Liver; miRNA

INTRODUCTION

In addition to modifying the composition of ductal bile by a series or reabsorptive and secretory mechanisms[1,2], cholangiocytes are the target of a group of chronic cholestatic liver diseases (i.e., cholangiopathies) such as primary sclerosing cholangitis (PSC) and primary biliary cholangitis (PBC), which are characterized by ductular reaction concomitant with biliary damage/senescence as well as subsequent activation of hepatic stellate cells (HSCs) and increased liver fibrosis[3–5]. During biliary injury, there is controversy whether ductular reaction exacerbates biliary damage/senescence or is a compensatory mechanism to repair the injured bile ducts and maintain proper biliary homeostasis[6].

Cellular senescence is a process that leads to irreversible cell cycle arrest in the G_0/G_1 phase, after cells are exposed to various stimuli such oncogenic stress, telomere shortening, protein aggregation, DNA damage, and mutations[7]. Many studies confirm that the increase in cellular senescence leads to various diseases, including diabetes, arteriosclerosis, osteoporosis, chronic

Address correspondence to Gianfranco Alpini, Ph.D., Professor of Medicine, VA Senior Research Scientist, Hickam Endowed Chair, Director, Indiana Center for Liver Research, Richard L. Roudebush VA Medical Center and Indiana University, Gastroenterology, Medicine, Cellular and Integrative Physiology, Biochemistry and Molecular Biology, 1481 W 10th Street, Dedication Wing – Room D-2004, Indianapolis, IN 46202, USA. Tel: 3179882337; E-mail: galpini@iu.edu *or* Gianfranco.alpini@va.gov

inflammatory, and neurodegenerative disorders[7]. Biliary senescence is a key hallmark of cholangiopathies, where injured cholangiocytes enter a senescence-associated secretory phenotype (SASP), secreting various cytokines, chemokines, and growth factors [e.g., transforming growth factor- 1 (TGF- -1), interleukin-6 (IL-6), IL-8, C–C motif chemokine ligand 2 (CCL2), and plasminogen activator inhibitor-1 (PAI-1)], which in turn further increase biliary senescence (by an autocrine loop) and activate HSCs, thereby increasing collagen deposition by paracrine mechanisms[4,8–11]. Among the well-known senescence markers p18, p15, p53, and PAI-1, Cdkn2a, p16[12] is a cyclin-dependent kinase inhibitor that plays a key role in the cell cycle regulation and is accumulated in senescent cells[13]. On the basis of these findings, we hypothesize that downregulation of p16 decreases biliary senescence/damage as well as ductular reaction and the activation of HSCs.

MicroRNAs (mRNAs) are small, noncoding RNA molecules involved in the inhibition of mRNA expression. miRNAs regulate a wide range of biological processes including physiological modulation or pathological disruption of various pathways[14]. Several studies have shown that miR-34a plays a key role in the regulation of cellular senescence in liver cells, such as hematopoietic stem cells (HSCs) and human umbilical cord vein endothelial cells[10,15,16]. Other studies have shown that the expression of miR-34a increases, whereas sirtuin 1 (SIRT1) expression decreases in a number of liver diseases, such as alcoholic liver injury, PBC, and nonalcoholic fatty liver disease (NAFLD)[16–20]. Based on these observations, we aimed to demonstrate that changes in the TGF- 1/miR-34a/SIRT1 axis modulate biliary senescence and its associated ductular reaction and the subsequent paracrine modulation of liver fibrosis.

MATERIALS AND METHODS

The rabbit antibodies against CDKN2A/p16INK4a (ab189034), TGF- 1 (ab92486), and collagen type 1 (Col1a1, ab34710) were purchased from Abcam (Cambridge, MA, USA). The rat antibody against cytokeratin-19 (CK19; a specific biliary marker)[21] was obtained from Developmental Studies Hybridoma Bank (Iowa City, IA, USA). 4 ,6-Diamidino-2-phenylindole (DAPI) was purchased from ThermoFisher Scientific (Waltham, MA, USA). The Sirius red staining kit was purchased from Abcam. Cellular Senescence Assay to detect SA- -galactosidase (SA- -GAL) activity was purchased from Millipore Sigma (Billerica, MA, USA). The mouse or human real-time polymerase chain reaction (PCR) primers, the RNeasy kit for total RNA extraction, and the reagents for real-time PCRs were purchased from Santa Cruz Biotechnology Inc. (Dallas, TX, USA). The enzyme-linked immunosorbent assay (ELISA) kits for the measurement of SASPs, the Mouse Cytokine ELISA Plate Array I (Colorimetric, EA-4005), was purchased from Signosis, Inc. (Santa Clara, CA, USA). We used the following mouse primers: SIRT1 (NM_001159589), Cdkn2a/p16 (NM_009877), Cdkn2b/p15 (NM_007670), Cdkn1a/p21 (NM_001111099), Cdkn2c/p18 (NM_007671), Cdkn1b/p27 (NM_009875), p53 (NM_001127233), Glb1, (NM_009752), TGF- 1 (NM_011577), TGF- R2 (NM_00937), Msln (NM_018857), platelet-derived growth factor- (PDGF ; NM_008808), tissue inhibitors of metalloproteinase 1 (TIMP1; NM_001044384), TIMP2 (NM_011594), TIMP3 (NM_011595), Col1a1 (NM_007742), -SMA/Acta2 (NM_007392), fibronectin-1 (Fn-1; NM_010233), MMP9 (NM_013599), Mki67 (NM_001081117), and GAPDH (housekeeping, NM_008084), and human primers: SIRT1 (NM_001142498) and glyceraldehyde-3-phosphate dehydrogenase (GAPDH; housekeeping, NM_001256799), all purchased from Qiagen (Venlo, Germany). The kit for iScript DNA Synthesis (cat. #170-8891) and iTaq Universal SYBR Green Supermix (cat. #172-5124) were obtained by Bio-Rad (Hercules, CA, USA). p16 Vivo-Morpholino and the respective mismatch Morpholino were obtained from Gene Tools, LLC (Philomath, OR). miRNA primers [hsa-miR34a (4427975: assay 000426) and U6 snRNA (4427975: assay 001973, housekeeping for miR-34a)] were purchased from ThermoFisher Scientific.

Animal Models

Male FVB/NJ wild-type (WT) and multidrug resistance gene 2 knockout ($Mdr2^{-/-}$) mice (PSC animal model, 12 weeks of age) were purchased from Jackson Laboratories (Bar Harbor, ME, USA); the $Mdr2^{-/-}$ were raised in our breeding colony. The animals were housed in a temperature-controlled environment (22°C) under 12:12-h light/dark cycles and had access to food and drinking water ad libitum. The in vivo experiments were performed in WT and $Mdr2^{-/-}$ mice treated with Vivo-Morpholino sequences against p16 (5 -CAGTGACCAAGAACCTGCGACCCA T-3') or mismatch Vivo-Morpholino sequences for p16 (5 -CAcTcACCAAcAACCTcCcACCCAT-3) [at the dose of 12.5 mg/kg body weight (BW)] by two tail vein injections (days 1 and 4); animals were euthanized at day 7. We have previously used Vivo-Morpholino treatment to downregulate hepatic expression of specific proteins in rodent models of cholestasis[21,22]. The animals were sacrificed after treatment with euthasol® (200–250 mg/kg BW) prior to collection of selected organs or liver perfusion. All the animal protocols were approved by the institutional animal care and use committee (IACUC) committee from both Baylor Scott & White Health and Indiana University Purdue University Indianapolis. Total liver tissues, isolated cholangiocytes, and cholangiocyte supernatant (after incubation for 4 h at 37°C of 10×10^6 isolated cholangiocytes)[11] were collected.

Purified Cholangiocytes and Intrahepatic Murine Cholangiocytes Lines (IMCLs)

Virtually pure cholangiocytes were isolated by immunoaffinity separation[21,23,24] using a monoclonal antibody [immunoglobulin M (IgM), a gift from Dr. Ronald A. Faris, Brown University, Providence, RI, USA] expressed by all intrahepatic cholangiocytes[24]. Cell number and viability were assessed by trypan blue exclusion. The in vitro studies were performed in our IMCLs, which display morphological, phenotypic, and functional characteristics similar to those of freshly isolated mouse cholangiocytes[21].

Human Studies

The collection and use of unidentified human samples (Table 1) from Dr. Suthat Liangpunsakul (Richard L. Roudebush L VA Medical Center and Indiana University, Indianapolis, IN, USA) was approved by the institutional review board (IRB) from Indiana University Purdue University Indianapolis. The collection of liver tissues from (i) healthy control patients with no known history of chronic liver diseases and collected during abdominal surgeries for various causes, and (ii) late stage PSC patients obtained from the explant during liver transplantation were obtained from Dr. Liangpunsakul; human samples were approved by the Indiana University Purdue University Indianapolis IRB. The human liver samples for mRNA analysis were collected through the Liver Tissue Procurement and Distribution System (Minneapolis, MN, USA)[25]. Written informed consent was received from participants prior to inclusion in the study.

Measurement of p16 Expression and Cellular Senescence in Liver Sections and Isolated Cholangiocytes

Following treatment of WT or Mdr2$^{-/-}$ mice with mismatch or p16 Vivo-Morpholino, we measured biliary senescence by immunofluorescence for p16 (costained with CK19) in frozen liver sections (10 m thick) and by immunohistochemistry for p16 in paraffin-embedded liver sections (4–5 m thick). Immunofluorescence staining was evaluated by the LEICA TSC SP5 X System (Leica Microsystems, Inc., Buffalo, Grove, IL, USA). Biliary senescence was further evaluated by (i) SA- -GAL staining in frozen liver sections (10 m thick) using the SA- -GAL commercially available kit (Millipore Sigma)[9] and (ii) mRNA expression of p15, p18, p21, p27, p53, and Glb1 by real-time PCR in cholangiocyte RNA (1 g). For the measurement of the SA- -GAL-positive areas, we used the Image-Pro Plus Version 6.0 software. Images of SA- -GAL and p16 immunostaining were captured by Olympus Image-Pro Plus Version 6.0 software (Olympus, Tokyo, Japan).

Measurement of Intrahepatic Bile Duct Mass (IBDM) and Liver Fibrosis

We measured IBDM by semiquantitative immunohistochemistry for CK19 in liver sections (4–5 m thick); 10 different fields were analyzed from three samples from three different animals from the selected groups of animals. Sections were examined using the Olympus Image Pro-Analyzer software 7.0 (Olympus). The data are expressed as area occupied by CK19-positive bile ducts/total area x 100[21].

Hepatic fibrosis was evaluated by Sirius red staining in paraffin-embedded liver sections (4–5 m thick); 10 different fields were analyzed from three samples from three different animals. Slides were scanned by a digital scanner (SCN400; Leica Microsystems Inc.) and quantified using Image-Pro Premier 9.1 (Media Cybernetics, Rockford, MD, USA). By immunofluorescence, we evaluated the immunoreactivity of Col1a1 in liver frozen sections (4–5 m thick) costained with CK19. Following

Table 1. Features of Healthy Control and PSC Patients

Group	Patient No.	Diagnosis	Gender	Age	Race	Origin
Control	1	Normal liver	N/A	N/A	N/A	Roudebush L VA Medical Center
Control	2	Normal liver	N/A	N/A	N/A	Roudebush L VA Medical Center
Control	3	Normal liver	N/A	N/A	N/A	Roudebush L VA Medical Center
Control	4	Normal liver	N/A	N/A	N/A	Roudebush L VA Medical Center
Control	5	Normal liver	N/A	N/A	N/A	Roudebush L VA Medical Center
PSC	1	Advanced-stage IV PSC	Male	60	White	Roudebush L VA Medical Center
PSC	2	PSC	N/A	N/A	N/A	Roudebush L VA Medical Center
PSC	3	PSC	Male	57	White	Roudebush L VA Medical Center
PSC	4	PSC	Male	33	White	Roudebush L VA Medical Center
PSC	5	PSC	Female	47	White	Roudebush L VA Medical Center
PSC	6	PSC	Male	42	White	Roudebush L VA Medical Center
PSC	7	PSC	Male	63	White	Roudebush L VA Medical Center

Human Samples are a gift of Dr. Suthat Liangpunsakul, Roudebush L VA Medical Center and Indiana University, Indianapolis, IN. PSC, primary sclerosing cholangitis.

immunofluorescence for Col1a1, images were evaluated by LEICA TSC SP5 X System (Leica Microsystems, Inc.). By real-time PCR, we measured the mRNA expression of Fn-1, -SMA, Col1a1, TIMP1, TIMP2, TIMP3, and MMP9 in isolated cholangiocytes from the selected groups of animals.

Measurement of the TGF-β1/miR-34a/SIRT1/p16 Axis in Mdr2$^{-/-}$ Mice and Human PSC Samples

Since Ingenuity Pathway Analysis software (Qiagen Bioinformatics, Valencia, CA, USA) (Fig. 1) indicates that TGF- 1 (an important factor modulating biliary senescence)[9] regulates miR-34a that alters SIRT1-depedent p16 expression (marker of senescence)[8,11], we evaluated by real-time PCR: (i) the expression of miR-34a in total liver samples from healthy control and late stage human PSC samples, and WT and Mdr2$^{-/-}$ mice treated with mismatch and p16 Vivo-Morpholinos, and (ii) the expression of SIRT1 in total liver samples from healthy control and late stage human PSC samples, and in total liver and isolated cholangiocytes from WT and Mdr2$^{-/-}$ mice and Mdr2$^{-/-}$ mice treated with p16 Vivo-Morpholinos. The expression levels of miR-34a were measured using TaqMan MicroRNA Reverse Transcription Kit and TaqMan MicroRNA Assay for hsa-mir-34a and U6 as reference (ThermoFisher Scientific) with ViiA 7 Real-Time PCR System (ThermoFisher Scientific). The rationale for these experiments is based on the following background: (i) TGF- 1 is upregulated in cholangiopathies including PSC[9,11], and (ii) the expression of miR-34a increases, whereas SIRT1 expression decreases in a number of liver diseases such as alcoholic liver injury, PBC, NAFLD, and in a rat model of CCl_4-induced liver fibrosis[7,16–20].

We evaluated by immunofluorescence TGF- 1 immunoreactivity in paraffin-embedded liver sections (10 m thick, costained with CK19) from the selected groups of animals. To detect SASP secretion in cholangiocyte supernatant, we measured the levels of cytokines present using the Mouse Cytokine ELISA Plate Array (Colorimetric, EA-4005; Signosis, Inc.), which permits monitoring of 24 mouse cytokines simultaneously.

In Vitro Studies in IMCLs: Effect of p16 Silencing on the Proliferative, Senescent, and Fibrotic Activity of IMCLs

To demonstrate the specificity of our findings to cholangiocytes, in vitro, IMCLs were treated with control vector or 1 pmol small interfering RNA against p16 (Qiagen, Venlo, Germany) for 24 h before evaluating the expression of proliferation (Ki-67), senescence (p16, p21, p15, p18, and p53), and fibrosis (Fn-1, TGF- 1, TGF- R2, TIMP1, MMP9, Msln, and PDGF) markers detected by real-time PCR.

Statistical Analysis

Data are expressed as mean ± standard error of the mean (SEM). Differences between groups were analyzed by Student's unpaired *t*-test when two groups were analyzed and analysis of variance (ANOVA) when more than two groups were analyzed using SPSS 22.0 software, followed by an appropriate post hoc test.

RESULTS

Measurement of Cellular Senescence

By immunofluorescence, the immunoreactivity of p16 increased in bile ducts (costained with CK19) from Mdr2$^{-/-}$ compared to WT mice, but decreased in bile ducts from Mdr2$^{-/-}$ mice treated with p16 Vivo-Morpholino compared to mismatch-treated Mdr2$^{-/-}$ mice (Fig. 2); no changes in biliary p16 immunoreactivity were observed

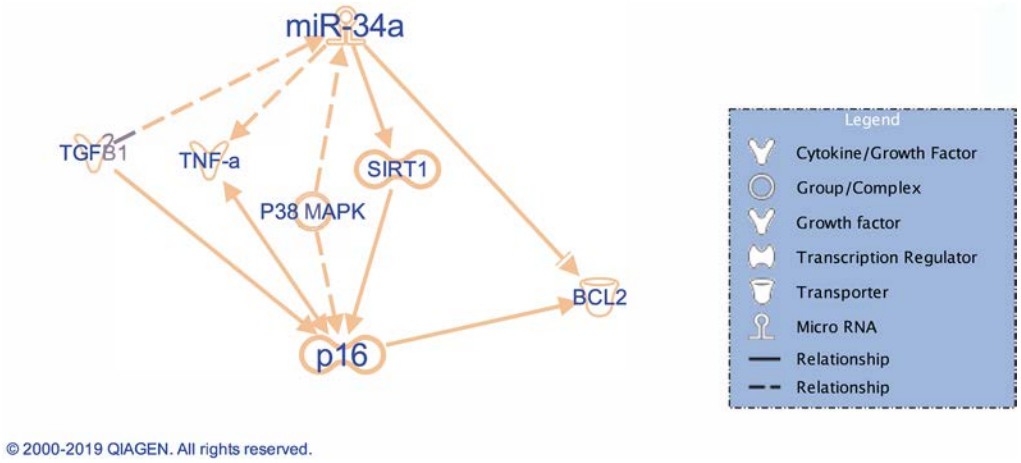

Figure 1. Representative diagram of the microRNA (miR)-34a/sirtuin 1 (SIRT1)/p16 axis outlined using the IPA pathway. The IPA-generated IPA supports our hypothesis showing that miR-34a modulates p16 (marker of senescence) through changes in SIRT1. Reproduced with permission from Qiagen.

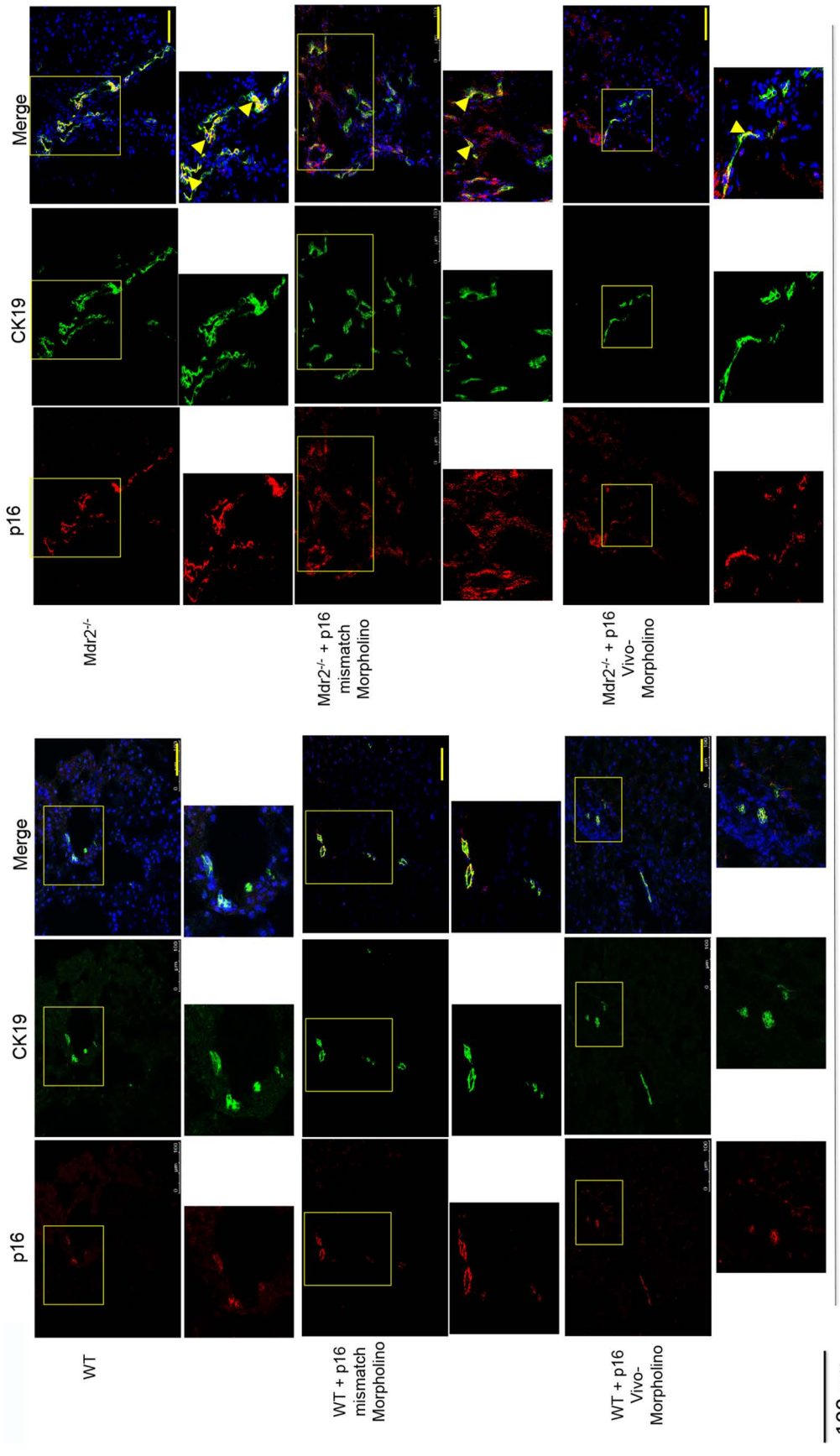

Figure 2. By immunofluorescence, we demonstrated increased immunoreactivity for p16 in bile ducts of $Mdr2^{-/-}$ mice and $Mdr2^{-/-}$ mice treated with p16 mismatch Morpholino compared to their respectively wild-type (WT) and $Mdr2^{-/-}$-treated mismatch Morpholino; p16 (red staining); CK19 (green staining); localization of p16 in bile ducts is indicated by yellow arrows. Nuclei were stained with 4 ,6-diamidino-2-phenylindole (DAPI). Scale bar: 100 m.

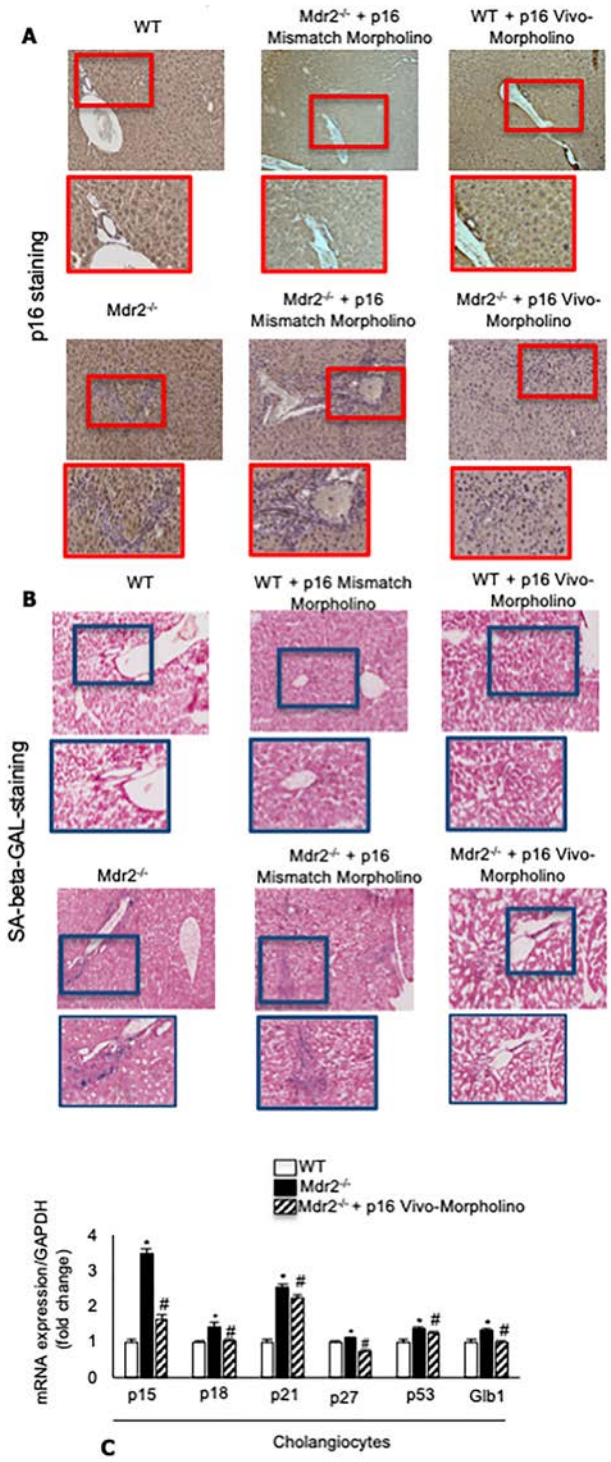

Figure 3. (A) There was enhanced p16 biliary immunoreactivity in Mdr2$^{-/-}$ compared to normal WT mice, which was decreased in Mdr2$^{-/-}$ mice treated with p16 mismatch Vivo-Morpholino compared to Mdr2$^{-/-}$ mice treated with mismatch Morpholino. Original magnification: 20×. (B) By SA- -galactosidase (SA- -GAL) staining in liver sections, there was enhanced biliary senescence in Mdr2$^{-/-}$ compared to WT mice that decreased in Mdr2$^{-/-}$ mice treated with p16 Vivo-Morpholino compared to mismatch-treated Mdr2$^{-/-}$ mice. Original magnification: 10×. (A, B) No changes in p16 immunoreactivity and biliary senescence immunoreactivity were observed between WT mice treated with p16 Vivo-Morpholino and mismatch control. (C) By real-time polymerase chain reaction (PCR), the mRNA expression of p15, p18, p21, p27, p53, and Glb1 increased in cholangiocytes from Mdr2$^{-/-}$ compared to WT mice, but decreased in Mdr2$^{-/-}$ mice treated with p16 Vivo-Morpholino compared to Mdr2$^{-/-}$ mice. Data are mean ± standard error of the mean (SEM) of three evaluations performed in a cumulative preparation of cholangiocytes from four mice *$p < 0.05$ versus WT mice. #$p < 0.05$ versus Mdr2$^{-/-}$ mice.

between WT mice treated with mismatch or p16 Vivo-Morpholino (Fig. 2).

Similarly, by immunohistochemistry, we demonstrated that the biliary p16 immunoreactivity increased in Mdr2$^{-/-}$ compared to normal WT mice, but decreased in Mdr2$^{-/-}$ mice treated with p16 mismatch Vivo-Morpholino compared to Mdr2$^{-/-}$ mice treated with mismatch Morpholino (Fig. 3A). By SA- -GAL staining in liver sections, there was enhanced biliary senescence in Mdr2$^{-/-}$ compared to WT mice, increased senescence that was reduced in Mdr2$^{-/-}$ mice treated with p16 Vivo-Morpholino compared to mismatch-treated Mdr2$^{-/-}$ mice (Fig. 3B); no changes in biliary p16 immunoreactivity and cellular senescence were observed between WT treated with p16 mismatch or Vivo-Morpholino (Fig. 3A and B). By real-time PCR, the mRNA expression of p15, p18, p21, p27, p53, and Glb1 increased in cholangiocytes from Mdr2$^{-/-}$ compared to WT mice, but decreased in Mdr2$^{-/-}$ mice treated with p16 Vivo-Morpholino compared to Mdr2$^{-/-}$ mice (Fig. 2C).

Measurement of IBDM and Liver Fibrosis

In agreement with previous studies[11], the administration of p16 Vivo-Morpholino markedly decreased IBDM compared to Mdr2$^{-/-}$ mice treated with mismatch Morpholino (Fig. 4); IBDM was similar among WT mice treated with p16 Vivo-Morpholino or the respective mismatch control (Fig. 4).

By Sirius red staining, there was increased collagen deposition in Mdr2$^{-/-}$ compared to WT mice, which decreased in Mdr2$^{-/-}$ mice treated with p16 Vivo-Morpholino compared to Mdr2$^{-/-}$ mice treated with mismatch-Morpholino; the extent of liver fibrosis was similar between WT mice treated with Vivo-Morpholino or their respective mismatch controls (Fig. 5A). By immunofluorescence, we demonstrated increased immunoreactivity of Col1a1 in Mdr2$^{-/-}$ compared to WT mice, which decreased in Mdr2$^{-/-}$ mice treated with p16 Vivo-Morpholino compared to Mdr2$^{-/-}$ mice treated with mismatch Morpholino; no difference in the immunoreactivity of Col1a1 was observed between WT mice treated with p16 Vivo-Morpholino and mismatch (Fig. 5B). By real-time PCR, we demonstrated that the expression of fibrosis markers Fn-1, Col1a1, -SMA, TIMP1, TIMP2, TIMP3, and MMP9 increased in Mdr2$^{-/-}$ mice compared to WT, but decreased in Mdr2$^{-/-}$ mice treated with p16 Vivo-Morpholino compared to Mdr2$^{-/-}$ mice (Fig. 5C).

Measurement of the TGF-β1/miR-34a/SIRT1/p16 Axis in Mdr2$^{-/-}$ Mice and Human PSC Samples

In total liver samples from human late-stage PSC patients, we demonstrated enhanced expression of miR-34a and reduced mRNA expression of SIRT1 compared to normal human samples (Fig. 6A and B). By real-time PCR, there was reduced levels of SIRT1 in isolated cholangiocytes and total liver from Mdr2$^{-/-}$ mice compared to WT mice, which returned to values similar to those of WT mice in Mdr2$^{-/-}$ mice treated with p16 Vivo-Morpholino (Fig. 6C). Furthermore, the expression of miR-34a increased in total liver samples from Mdr2$^{-/-}$ mice and Mdr2$^{-/-}$ mice treated with p16 mismatch Morpholinos compared to WT mice, but decreased in Mdr2$^{-/-}$ mice treated with p16 Vivo-Morpholino compared to Mdr2$^{-/-}$ mice and Mdr2$^{-/-}$ mice treated with p16 mismatch Morpholino (Fig. 6C); no changes in miR-34a expression were observed between WT mice and WT mice treated with mismatch or p16 Vivo-Morpholino (Fig. 6C).

We demonstrated increased biliary immunoreactivity of TGF- 1 (in liver sections) and enhanced levels of SASPs in cholangiocyte supernatant from Mdr2$^{-/-}$ mice compared to WT mice, which decreased in Mdr2$^{-/-}$ mice treated with p16 Vivo-Morpholino compared to Mdr2$^{-/-}$ mice (Fig. 7A and B). No differences in TGF- 1 immunoreactivity were observed in normal WT mice treated with p16 Vivo-Morpholino and mismatch Morpholino (Fig. 7A).

In Vitro Studies in IMCLs: Effect of p16 Silencing on the Proliferative, Senescent, and Fibrotic Activity of IMCLs

In p16-silenced IMCLs, there was reduced mRNA expression of proliferation (Ki-67), senescence (p16, p21, p15, p18, and p53), and fibrosis (Fn-1, TGF- 1, TGF- -R2, TIMP1, MMP9, Msln, and PDGF) markers compared to control IMCLs (Fig. 8A and B).

DISCUSSION

The study focuses on the role of the TGF- 1/miRNA-34a/SIRT1/p16 axis in the regulation of biliary damage/senescence and liver fibrosis in the Mdr2$^{-/-}$ mouse model of PSC, as well as total liver specimen from late stage human PSC patients. Specifically, we found that biliary senescence was increased in Mdr2$^{-/-}$ compared to WT mice, but decreased in Mdr2$^{-/-}$ mice treated with p16 Vivo-Morpholino compared to mismatch-treated Mdr2$^{-/-}$ mice. The reduction in biliary senescence was associated with decreased levels of SASP cytokines concomitant with diminished IBDM and liver fibrosis. In Mdr2$^{-/-}$ mice, there was decreased expression of SIRT1 (in isolated cholangiocytes and total liver samples) but increased expression of miR-34 (in total liver samples) compared to WT mice, changes that were reversed in Mdr2$^{-/-}$ mice treated with p16 Vivo-Morpholino. Parallel with the changes observed in Mdr2$^{-/-}$ mice, we demonstrated increased expression of microRNA-34a but decreased expression of SIRT1 in total liver samples from late stage human PSC patients compared to healthy control samples.

Cholangiocyte proliferation (i.e., ductular reaction) and biliary damage/senescence are typical hallmarks of

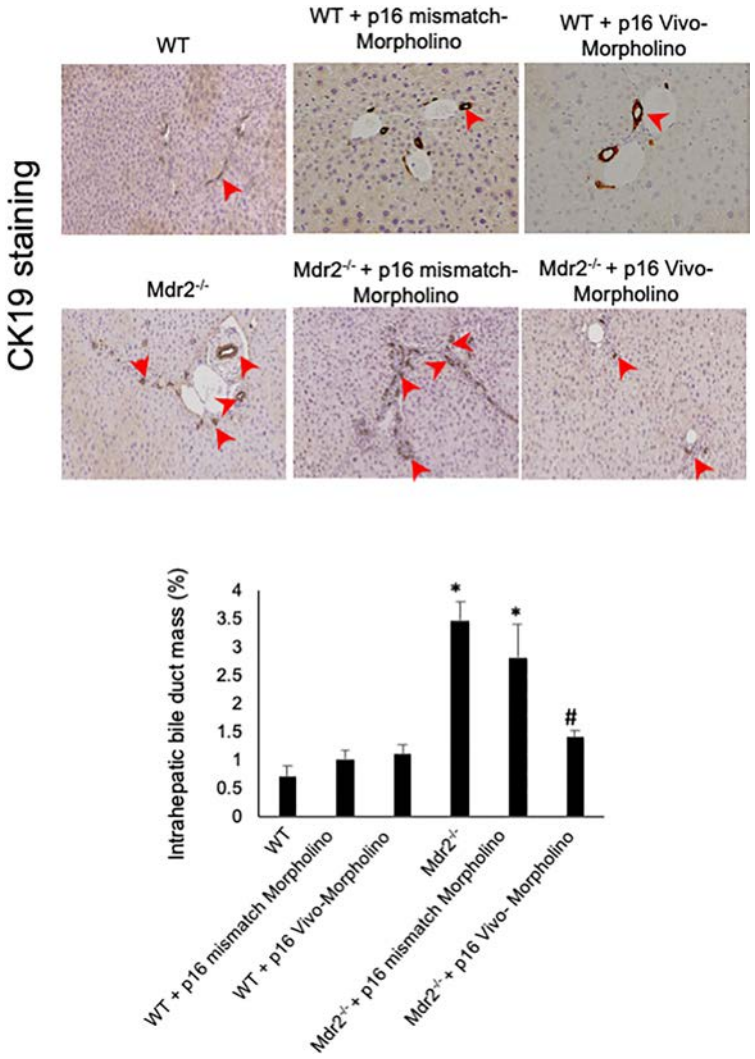

Figure 4. IBDM increased in Mdr2$^{-/-}$ compared to WT mice, but decreased in Mdr2$^{-/-}$ mice treated with p16 Vivo-Morpholino mice compared to their respective mismatched controls. In Mdr2$^{-/-}$ mice, IBDM increased significantly compared to WT mice; however, the administration of p16 Vivo-Morpholino markedly decreased IBDM compared to Mdr2$^{-/-}$ mice treated with mismatch Morpholino; IBDM was similar among WT mice treated with p16 Vivo-Morpholino or the respective mismatch control. Bile ducts are indicated by red arrows. Ten different fields from three samples from three different animals were analyzed. Original magnification: 20×. *$p < 0.05$ versus WT mice. #$p < 0.05$ versus Mdr2$^{-/-}$ mice.

cholestatic liver diseases, such as extrahepatic cholestasis [mimicked in rodents by extrahepatic bile duct ligation (BDL)], PSC, and PBC, as well as in mice subjected to high-fat diet feeding and patients with NAFLD[6,9,26–31]. In human cholestatic liver diseases and animal models of cholestasis and biliary injury/senescence (characterized by inflammation, biliary damage, and liver fibrosis)[6], there is controversy whether ductular reaction has a negative role in sustaining biliary/liver damage or is a compensatory, beneficial mechanism (during the progression of cellular senescence) to maintain proper biliary homeostasis during liver injury[6]. This notion is highlighted by our current results showing that inhibition of biliary senescence (by administration of p16 Vivo-Morpholino) reduces IBDM (ductular reaction) in Mdr2$^{-/-}$ mice, a finding that disagrees with previous studies that enhanced cellular senescence is associated with irreversible growth arrest[32,33].

To explain why the decrease in biliary senescence is associated with reduced ductular reaction, we propose that targeting of a specific subset of senescent cholangiocytes (after treatment p16 Vivo-Morpholino) decreases the release of toxic biliary SASPs that, in turn, induces a paracrine decrease (i.e., interaction between senescent and nonsenescent cholangiocytes)[34] in the compensatory ductular reaction[6], thus reducing IBDM. We propose that large

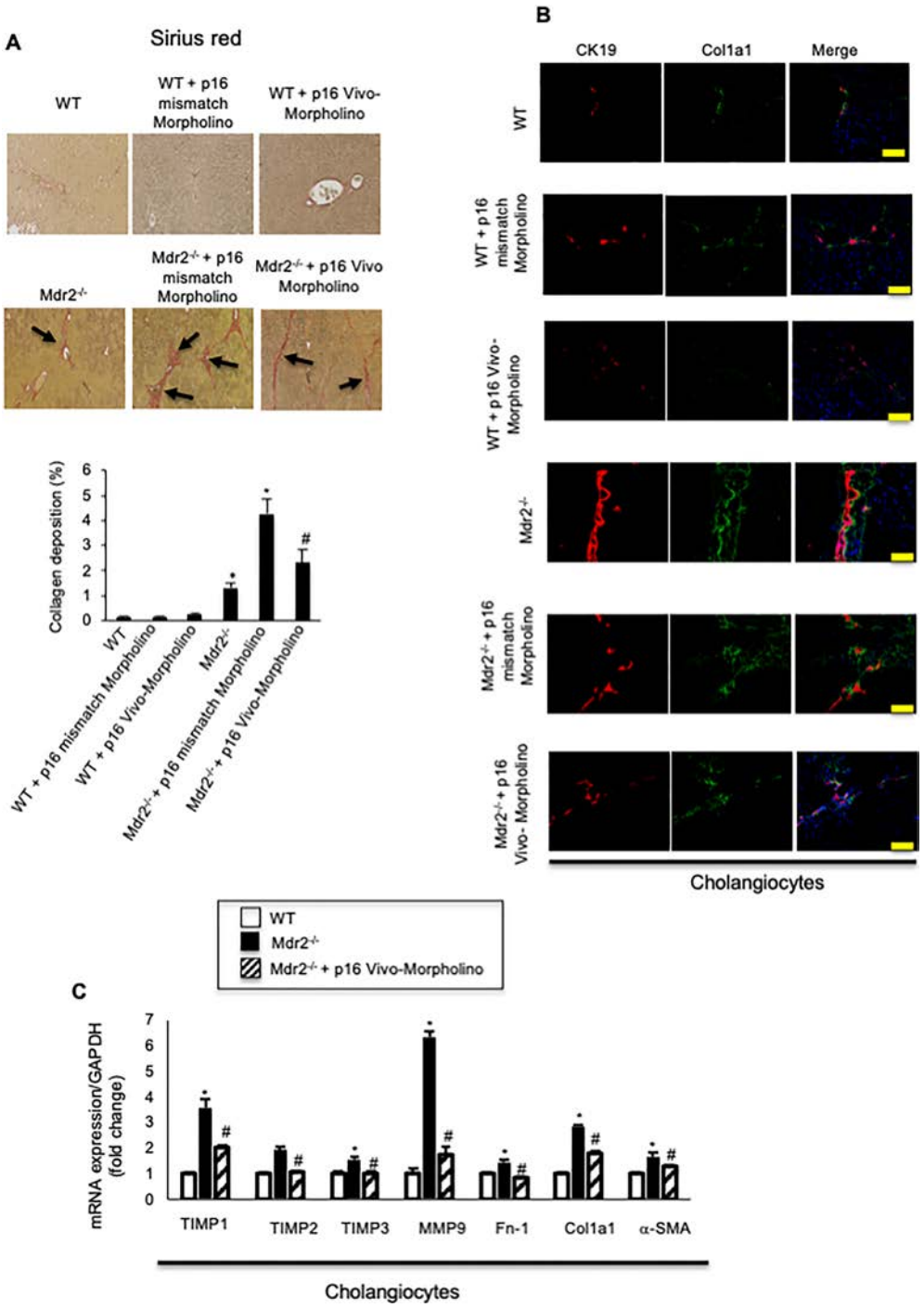

Figure 5. (A) There was increased collagen deposition in Mdr2$^{-/-}$ compared to WT mice, which decreased in Mdr2$^{-/-}$ mice treated with p16 Vivo-Morpholino compared to Mdr2$^{-/-}$ mice treated with mismatch Morpholino. Ten different fields from three samples from three different animals were analyzed. Original magnification: 20×. *$p < 0.05$ versus WT mice. #$p < 0.05$ versus Mdr2$^{-/-}$ mice. Black arrows show collagen deposition around bile ducts. (B) By immunofluorescence, there was increased immunoreactivity of Col1a1 in Mdr2$^{-/-}$ compared to WT mice, which decreased in Mdr2$^{-/-}$ mice treated with p16 Vivo-Morpholino sequences compared to Mdr2$^{-/-}$ mice treated with mismatch Morpholino. Col1a1 (green staining); CK19 (red staining); nuclei were stained with DAPI; scale bar: 100 m. *$p < 0.05$ versus WT mice. #$p < 0.05$ versus Mdr2$^{-/-}$ mice. (A, B). There were no changes in liver fibrosis between WT mice treated with p16 mismatch Morpholino and p16 Vivo-Morpholino. (C) By real-time PCR, the mRNA expression of fibrosis markers Fn-1, Col1a1, a-SMA, TIMP1, TIMP2, TIMP3, and MMP9 increased in cholangiocytes from Mdr2$^{-/-}$ compared to WT mice, but decreased in Mdr2$^{-/-}$ mice treated with p16 Vivo-Morpholino compared to Mdr2$^{-/-}$ mice. Data are mean ± SEM of three evaluations performed in a cumulative preparation of cholangiocytes from four mice. *$p < 0.05$ versus WT mice. #$p < 0.05$ versus Mdr2$^{-/-}$ mice.

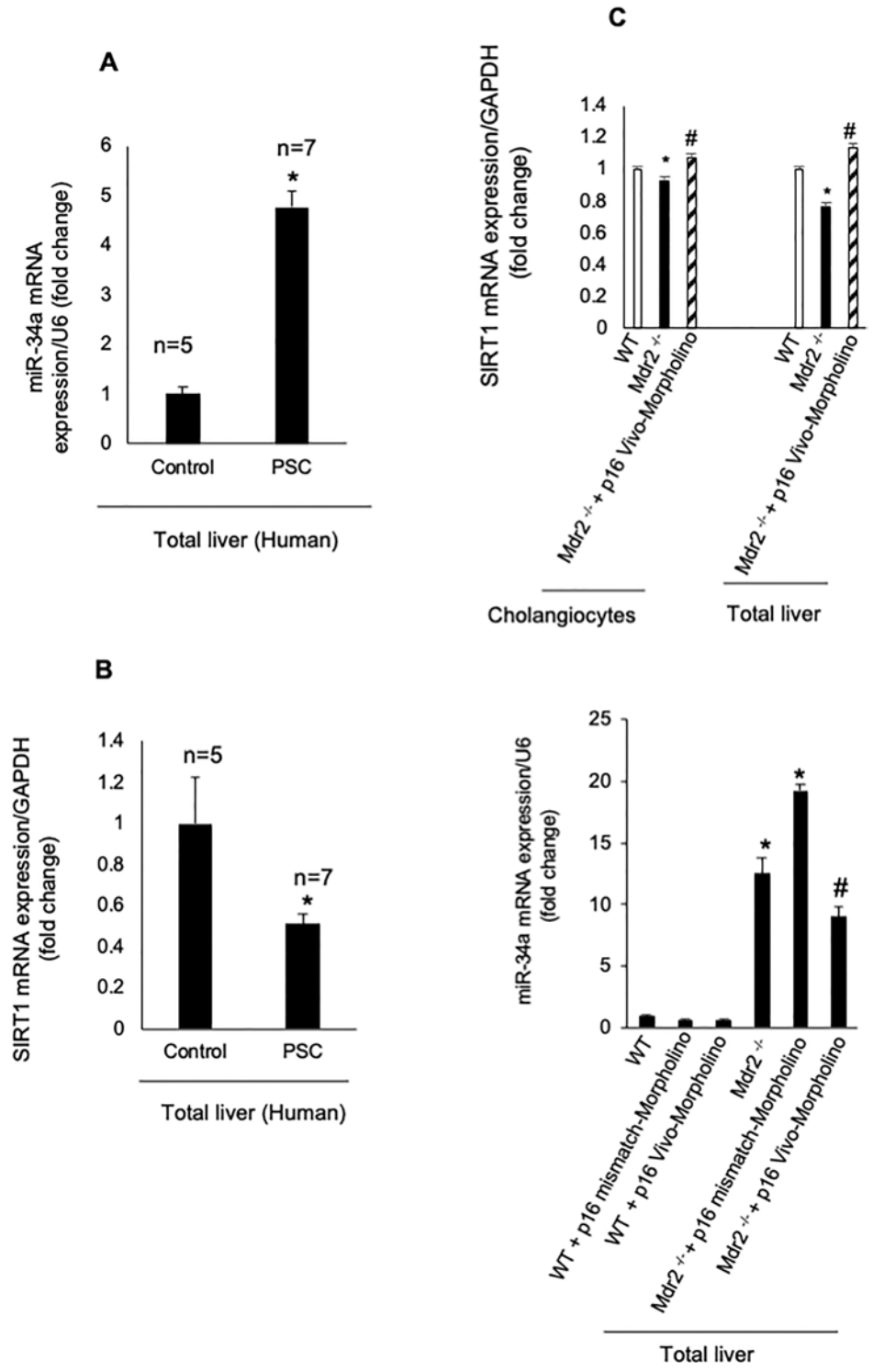

Figure 6. (A, B) In human PSC samples, we demonstrated (i) enhanced expression of miR-34a (in total liver samples) and (ii) reduced mRNA expression of SIRT1 in total liver samples compared to normal human samples. Data are mean ± SEM from seven late stage PSC patients and five normal human controls. *$p < 0.05$ versus control human samples. (C) By real-time PCR, there was reduced levels of SIRT1 in isolated cholangiocytes and total liver from $Mdr2^{-/-}$ mice compared to WT mice, which returned to values similar to those of WT mice in $Mdr2^{-/-}$ mice treated with p16 Vivo-Morpholino. Data are mean ± SEM of three evaluations performed in a cumulative preparation of cholangiocytes from four mice. Data are mean ± SEM of three evaluations performed in three different total liver samples from three different mice. *$p < 0.05$ versus WT mice, #$p < 0.05$ versus $Mdr2^{-/-}$ mice.

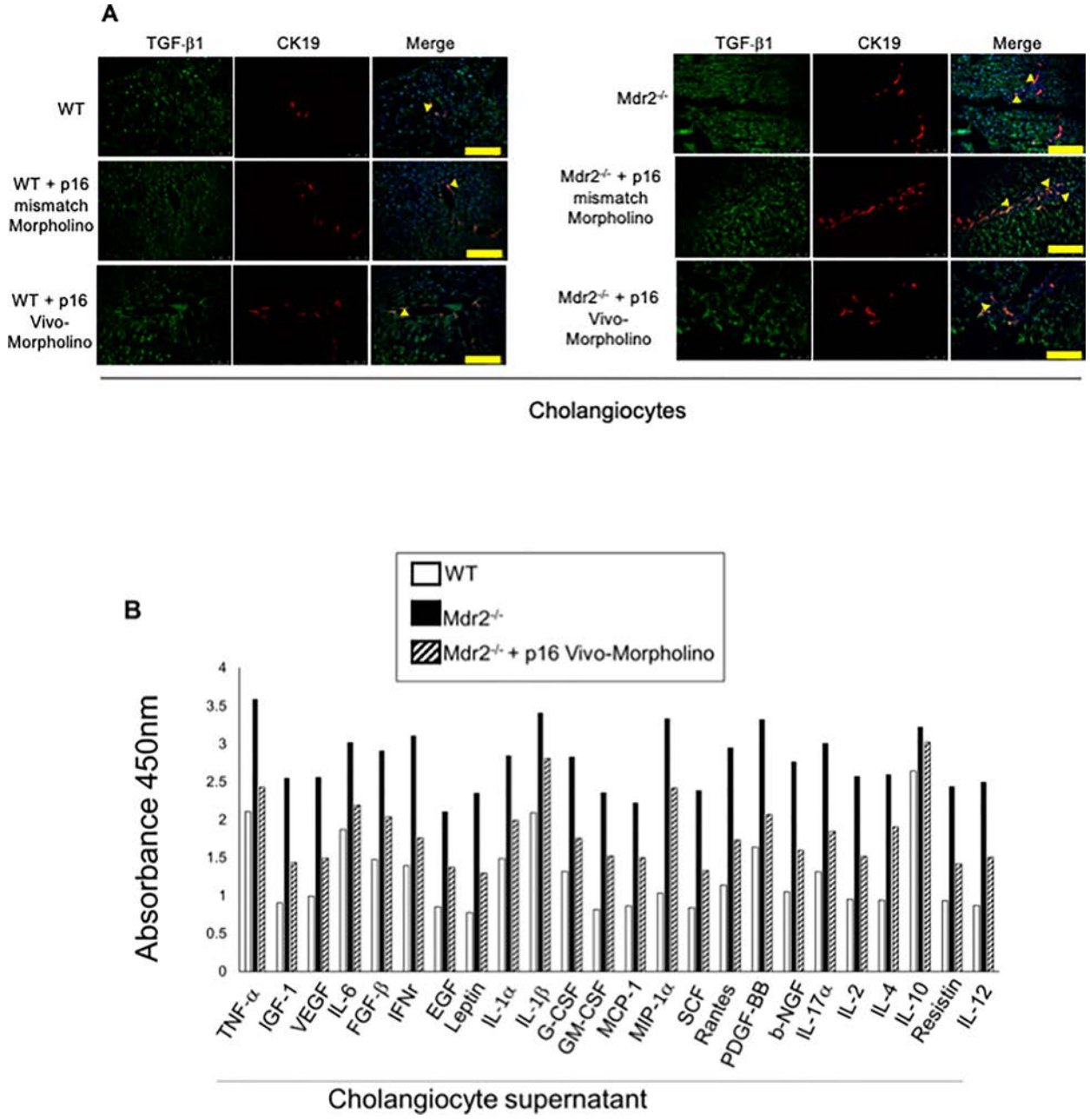

Figure 7. (A) By immunofluorescence, we demonstrated increased immunoreactivity for transforming growth factor- 1 (TGF- 1) in bile ducts of Mdr2$^{-/-}$ mice and Mdr2$^{-/-}$ mice treated with p16 mismatch Morpholino compared to their respective WT and Mdr2$^{-/-}$ treated mismatch Morpholino; TGF- 1 (green staining); CK19 (red staining); localization of TGF- 1 in bile ducts is indicated by yellow arrows. Nuclei were stained with DAPI. Scale bar: 100 m. (B) There was increase in SASPs levels in cholangiocyte supernatant from Mdr2$^{-/-}$ mice (compared to WT mice), parameters that all decreased in Mdr2$^{-/-}$ mice treated with p16 Vivo-Morpholino compared to Mdr2$^{-/-}$ mice. Evaluation is the result of cumulative preparation of cholangiocytes from four mice.

cholangiocytes are likely the cell types targeted by p16 Vivo-Morpholino. This is based on unpublished observations from our group showing that cAMP-dependent, large (but not small) cholangiocytes display SASP phenotypes (Glaser and Alpini, unpublished observations, 2020). This notion is supported by our previous studies showing that (i) in the cholestatic model of BDL, only large cholangiocytes proliferate[23,35], and (ii) large but not small cholangiocytes are damaged by pathological maneuverers such as acute carbon tetrachloride administration or chronic -aminobutyric acid administration leading, maneuvers that lead to increased small duct mass[36,37].

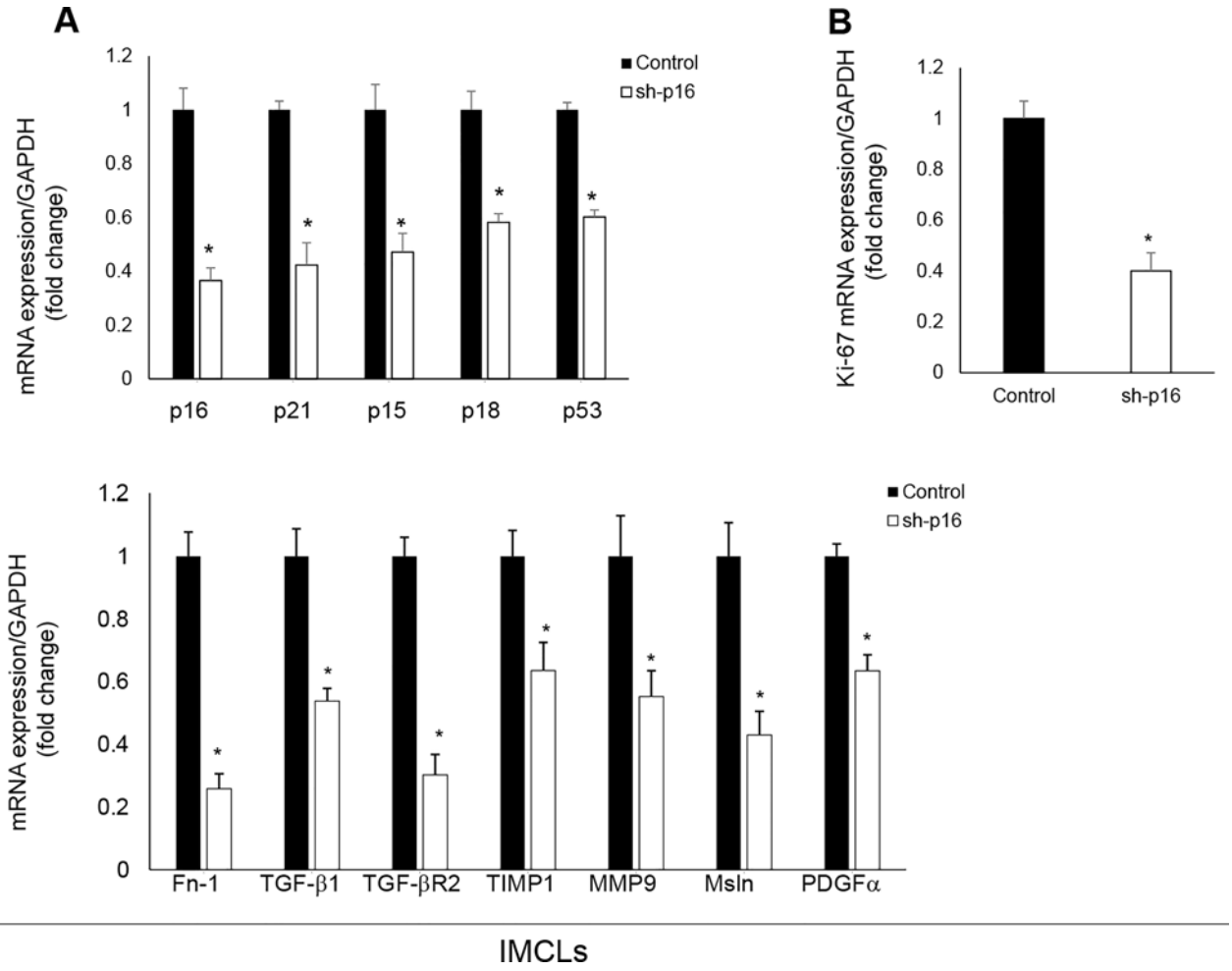

Figure 8. (A, B) In p16-silenced IMCLs, there was reduced expression of senescence, fibrosis, and proliferation (Ki-67) mRNAs compared to control IMCLs. Data are mean ± SEM of $n = 3$ from three preparations of IMCLs. *$p < 0.05$ versus IMCLs.

In future experiments in Mdr2$^{-/-}$ mice, we plan to evaluate whether large cholangiocytes are the target of p16 and whether the decrease in large cholangiocyte mass (following administration of p16 Vivo-Morpholino) is associated with enhanced proliferation of small cholangiocytes. A shortcoming of our in vivo studies is represented by the fact that we did not demonstrate whether the p16 Vivo-Morpholinos may target other liver cells such as hepatocytes and Kupffer cells (but not HSCs) in addition to cholangiocytes. We exclude the possibility that p16 Vivo-Morpholino may interact with HSCs, since inhibition of HSC senescence results in increased liver fibrosis[9], opposite to what we have shown in our results. However, supporting the specificity of our data to cholangiocytes, we show in in vitro studies that inhibition of p16 reduces biliary senescence, proliferation, as well as fibrogenic activity. Supporting our findings, there was a concomitant increase in ductular reaction and biliary senescence in both BDL WT and Mdr2$^{-/-}$ mice, phenotypes that were reduced by genetic knockout of the neurokinin receptor (NK1R) in BDL mice and by administration of an NK1R antagonist to Mdr2$^{-/-}$ mice[9]. In support of this concept, the SR antagonist, Sec 5-27, inhibits ductular reaction and biliary senescence (by an autocrine loop by interaction with a basolateral receptor expressed only by cholangiocytes) and liver fibrosis by a paracrine pathway through decreased TGF- 1 biliary secretion mouse models of PSC and early stage PBC[11,26].

Consistent with the concept that enhanced levels of SASPs (in Mdr2$^{-/-}$ and human PSC samples) are key stimulatory factors of cholangiocyte senescence (by an autocrine loop) and activation of HSCs (by paracrine mechanisms), we have shown that the expression and levels of several cytokines (including TGF- 1, IL-6, IL-8, CCL2, and PAI-1) were increased in Mdr2$^{-/-}$ mice, but decreased in Mdr2$^{-/-}$ mice treated with p16 Vivo-Morpholinos. Among the SASPs evaluated, a number of studies have shown that TGF- 1 is a key player

in the modulation of biliary damage and liver fibrosis. For example, during early chronic liver allograft rejection, there is enhanced expression/release of TGF- 1 that increases biliary senescence ablating the compensatory ductular reaction in response to liver injury[38]. Other studies have shown that senescent cholangiocytes release TGF- 1, which induces senescence in surrounding cholangiocytes and subsequent recruitment of myofibroblasts and macrophages, causing activation of HSCs and collagen deposition in several models of biliary senescence induced by BDL, conditional deletion of Mdm2 in bile ducts, and the Mdr2$^{-/-}$ mouse model of PSC[11,34,39]. Furthermore, other studies have shown that interferon IL-6, interferon- (INF-), INF- , and INF- promote cellular senescence of cholangiocytes[40], and higher levels of SASPs (e.g., IL-6, IL-8, CCL2, and PAI-1) were increased in human PSC cholangiocytes[4]. Consistent with our findings, senescent cholangiocytes secrete CCL2 and CX3CL1 that promote infiltration of corresponding CCR2- and CX3CR1-expressing cells, exacerbating inflammation of bile ducts in PBC[41,42]. Moreover, senescent endotoxic animals exhibit higher circulating levels of TNF- , IL-1 , IL-6, IL-10, and RANTES compared to young endotoxic rats[43]. Taken together, the data suggested that in vivo downregulation of p16 (by administration of Vivo-Morpholinos) reduces the levels of specific biliary SASPs (that have been shown to activate HSCs) in Mdr2$^{-/-}$ mice, thereby reducing liver fibrosis. While the paracrine role of some of these biliary SASPs in the activation of HSCs has been demonstrated, more direct studies are necessary to determine whether these biliary SASPs (e.g., basic fibroblast growth factor, epidermal growth factor, and resistin)[17,44–46], expressed in HSCs and stimulating liver fibrosis by directly interacting with HSCs, increase liver fibrosis by paracrine pathways.

We next evaluated the role of the miR-34a/SIRT1 axis in the regulation of biliary senescence and the subsequent paracrine modulation of liver fibrosis. The rationale for these studies is based on the background that the expression of miR-34a increases, whereas SIRT1 expression decreases in a number of liver diseases such as PBC and NAFLD[17,18], studies that agree with our

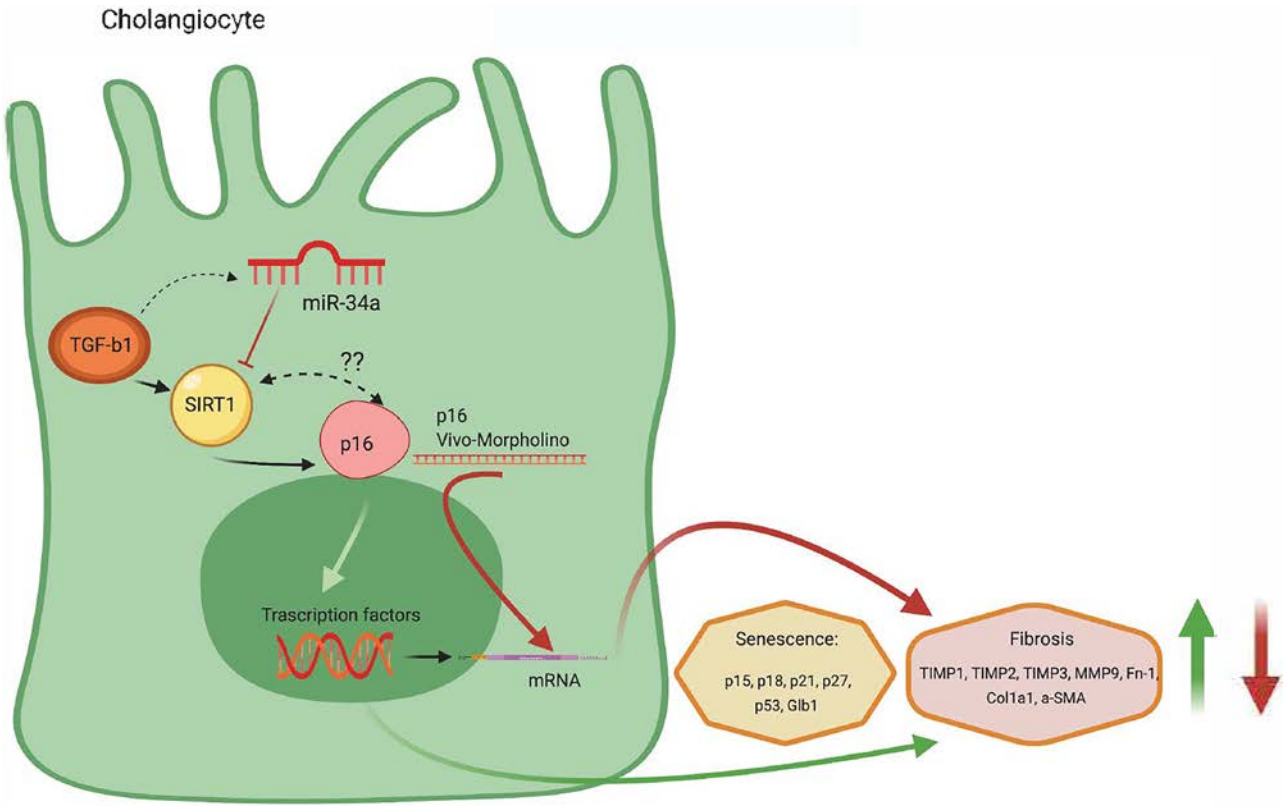

Figure 9. We depicted a working model illustrating the role of the TGF- 1/miR-34a/SIRT1/p16 axis in regulating biliary proliferation/senescence and paracrine activation of hepatic stellate cells (HSCs) with subsequent increase in liver fibrosis. TGF- 1 stimulates miR-34a and inhibits SIRT1, activating p16 that stimulates the transcription of the senescence (p15, p18, p21, p27, p53, and Glb1) and fibrosis (TIMP1, TIMP2, MMP9, Fn-1, Col1a1, and -SMA) markers. Also, TGF- 1 stimulates directly p16 and activates the fibrosis and senescence gene transcription. The cartoon suggests a link between TGF- 1, p16, and SIRT1 through a feedback mechanism. Created with BioRender. com.

current findings related to the expression of the miR-34a/SIRT1 axis in Mdr2$^{-/-}$ mice and late stage human PSC samples. Consistent with this concept, a study has shown that (i) the expression levels of SIRT1 was decreased in a mouse model of PBC, and (ii) activation of SIRT1 signaling ameliorates PBC and NAFLD phenotypes[17,47]. Supporting our findings, miR-34a/SIRT1-dependent cellular senescence has been demonstrated in other cell types such as HSCs (during alcohol-induced liver damage) and human umbilical cord vein endothelial cells[15,16]. Taken together, our in vivo and in vitro data demonstrated the key role of the miR-34a/SIRT1 axis in regulating biliary senescence (by an autocrine loop) and liver fibrosis by a paracrine mechanism. A shortcoming of our study is represented by the fact that we did not evaluate the role of the miR-34a/SIRT1 axis in modulating biliary apoptosis since biliary senescence and apoptosis may display a dueling or a complementary pattern[48]. In conclusion, we provide evidence that modulation of miR-34a/SIRT1/p16 signaling may be important for the management of biliary damage/senescence and associated ductular reaction and subsequent liver fibrosis during the development and progression of human PSC (Fig. 9).

ACKNOWLEDGMENTS: This work was supported by the Hickam Endowed Chair, Gastroenterology, Medicine, Indiana University and the Indiana University Health – Indiana University School of Medicine Strategic Research Initiative, the VA Merit awards to Dr. Alpini (5I01BX000574), Dr. Francis (1I01BX003031), and Dr. Meng (1I01BX001724) from the United States Department of Veteran's Affairs, Biomedical Laboratory Research and Development Service, and NIH grants DK108959 and DK119421 (H.F.), DK054811, DK076898, DK107310, DK110035, DK062975, AA025997, and AA025157 to Drs. Alpini, Meng, and Glaser, AA026385 (Z.Y.), and partly from the BaylorScott & White Research Institute. This material is the result of work supported by resources at the Central Texas Veterans Health Care System, Temple, TX, Richard L. Roudebush VA Medical Center, Indianapolis, IN, and Medical Physiology, Medical Research Building, Temple, TX. The views expressed in this article are those of the authors and do not necessarily represent the views of the Department of Veterans Affairs.

REFERENCES

1. Alpini G, Lenzi R, Sarkozi L, Tavoloni N. Biliary physiology in rats with bile ductular cell hyperplasia. Evidence for a secretory function of proliferated bile ductules. J Clin Invest. 1988;81(2):569–78.
2. Kanno N, LeSage G, Glaser S, Alpini G. Regulation of cholangiocyte bicarbonate secretion. Am J Physiol Gastrointest Liver Physiol. 2001;281(3):G612–25.
3. Glaser S, Gaudio E, Miller T, Alvaro D, Alpini G. Cholangiocyte proliferation and liver fibrosis. Expert Rev Mol Med. 2009;11:e7.
4. Tabibian JH, O'Hara SP, Splinter PL, Trussoni CE, LaRusso NF. Cholangiocyte senescence by way of N-ras activation is a characteristic of primary sclerosing cholangitis. Hepatology 2014;59(6):2263–75.
5. Nakanuma Y, Sasaki M, Harada K. Autophagy and senescence in fibrosing cholangiopathies. J Hepatol. 2015;62(4):934–45.
6. Sato K, Marzioni M, Meng F, Francis H, Glaser S, Alpini G. Ductular reaction in liver diseases: Pathological mechanisms and translational significances. Hepatology 2019;69(1):420–30.
7. Tchkonia T, Zhu Y, van Deursen J, Campisi J, Kirkland JL. Cellular senescence and the senescent secretory phenotype: Therapeutic opportunities. J Clin Invest. 2013; 123(3):966–72.
8. Zhou T, Wu N, Meng F, Venter J, Giang TK, Francis H, Kyritsi K, Wu C, Franchitto A, Alvaro D and others. Knockout of secretin receptor reduces biliary damage and liver fibrosis in Mdr2($^{-/-}$) mice by diminishing senescence of cholangiocytes. Lab Invest. 2018;98(11):1449–64.
9. Wan Y, Meng F, Wu N, Zhou T, Venter J, Francis H, Kennedy L, Glaser T, Bernuzzi F, Invernizzi P, et al. Substance P increases liver fibrosis by differential changes in senescence of cholangiocytes and hepatic stellate cells. Hepatology 2017;66(2):528–41.
10. Meng L, Quezada M, Levine P, Han Y, McDaniel K, Zhou T, Lin E, Glaser S, Meng F, Francis H, et al. Functional role of cellular senescence in biliary injury. Am J Pathol. 2015;185(3):602–9.
11. Wu N, Meng F, Invernizzi P, Bernuzzi F, Venter J, Standeford H, Onori P, Marzioni M, Alvaro D, Franchitto A, et al. The secretin/secretin receptor axis modulates liver fibrosis through changes in transforming growth factor-beta1 biliary secretion in mice. Hepatology 2016;64(3):865–79.
12. Baker DJ, Wijshake T, Tchkonia T, LeBrasseur NK, Childs BG, van de Sluis B, Kirkland JL, van Deursen JM. Clearance of p16Ink4a-positive senescent cells delays ageing-associated disorders. Nature 2011;479(7372):232–6.
13. Zhao R, Choi BY, Lee MH, Bode AM, Dong Z. Implications of genetic and epigenetic alterations of CDKN2A (p16(INK4a)) in cancer. EBioMedicine 2016;8:30–9.
14. Feliciano A, Sanchez-Sendra B, Kondoh H, Lleonart ME. MicroRNAs regulate key effector pathways of senescence. J Aging Res. 2011;2011:205378.
15. Ito T, Yagi S, Yamakuchi M. MicroRNA-34a regulation of endothelial senescence. Biochem Biophys Res Commun. 2010;398(4):735–40.
16. Wan Y, McDaniel K, Wu N, Ramos-Lorenzo S, Glaser T, Venter J, Francis H, Kennedy L, Sato K, Zhou T, et al. Regulation of cellular senescence by miR-34a in alcoholic liver injury. Am J Pathol. 2017;187(12):2788–98.
17. Li Y, Xi Y, Tao G, Xu G, Yang Z, Fu X, Liang Y, Qian J, Cui Y, Jiang T. Sirtuin 1 activation alleviates primary biliary cholangitis via the blocking of the NF-kappaB signaling pathway. Int Immunopharmacol. 2020;83:106386.
18. Wu T, Liu YH, Fu YC, Liu XM, Zhou XH. Direct evidence of sirtuin downregulation in the liver of non-alcoholic fatty liver disease patients. Ann Clin Lab Sci. 2014;44(4):410–8.
19. Tan Y, Pan T, Ye Y, Ge G, Chen L, Wen D, Zou S. Serum microRNAs as potential biomarkers of primary biliary cirrhosis. PLoS One 2014;9(10):e111424.
20. Wasik U, Milkiewicz M, Kempinska-Podhorodecka A, Milkiewicz P. Protection against oxidative stress mediated by the Nrf2/Keap1 axis is impaired in primary biliary cholangitis. Sci Rep. 2017;7:44769.
21. Glaser S, Meng F, Han Y, Onori P, Chow BK, Francis H, Venter J, McDaniel K, Marzioni M, Invernizzi P and others. Secretin stimulates biliary cell proliferation by regulating

expression of microRNA 125b and microRNA let7a in mice. Gastroenterology 2014;146(7):1795–808.e12.
22. Kyritsi K, Meng F, Zhou T, Wu N, Venter J, Francis H, Kennedy L, Onori P, Franchitto A, Bernuzzi F and others. Knockdown of hepatic gonadotropin-releasing hormone by Vivo-Morpholino decreases liver fibrosis in multidrug resistance gene 2 knockout mice by down-regulation of miR-200b. Am J Pathol. 2017;187(7):1551–65.
23. Glaser S, Lam IP, Franchitto A, Gaudio E, Onori P, Chow BK, Wise C, Kopriva S, Venter J, White M and others. Knockout of secretin receptor reduces large cholangiocyte hyperplasia in mice with extrahepatic cholestasis induced by bile duct ligation. Hepatology 2010;52(1):204–14.
24. Ishii M, Vroman B, LaRusso NF. Isolation and morphologic characterization of bile duct epithelial cells from normal rat liver. Gastroenterology 1989;97(5):1236–47.
25. Zhang Y, Xu N, Xu J, Kong B, Copple B, Guo GL, Wang L. E2F1 is a novel fibrogenic gene that regulates cholestatic liver fibrosis through the Egr-1/SHP/EID1 network. Hepatology 2014;60(3):919–30.
26. Kennedy L, Francis H, Invernizzi P, Venter J, Wu N, Carbone M, Gershwin ME, Bernuzzi F, Franchitto A, Alvaro D, et al. Secretin/secretin receptor signaling mediates biliary damage and liver fibrosis in early-stage primary biliary cholangitis. FASEB J. 2019;33(9):10269–79.
27. Meadows V, Kennedy L, Hargrove L, Demieville J, Meng F, Virani S, Reinhart E, Kyritsi K, Invernizzi P, Yang Z and others. Downregulation of hepatic stem cell factor by Vivo-Morpholino treatment inhibits mast cell migration and decreases biliary damage/senescence and liver fibrosis in Mdr2($^{-/-}$)mice. Biochim Biophys Acta Mol Basis Dis. 2019;1865(12):165557.
28. Papatheodoridi AM, Chrysavgis L, Koutsilieris M, Chatzigeorgiou A. The role of senescence in the development of nonalcoholic fatty liver disease and progression to nonalcoholic steatohepatitis. Hepatology 2020;71(1):363–74.
29. Aravinthan AD, Alexander GJM. Senescence in chronic liver disease: Is the future in aging? J Hepatol. 2016;65 (4):825–34.
30. Natarajan SK, Ingham SA, Mohr AM, Wehrkamp CJ, Ray A, Roy S, Cazanave SC, Phillippi MA, Mott JL. Saturated free fatty acids induce cholangiocyte lipoapoptosis. Hepatology 2014;60(6):1942–56.
31. Kennedy L, Hargrove L, Demieville J, Bailey JM, Dar W, Polireddy K, Chen Q, Nevah Rubin MI, Sybenga A, DeMorrow S and others. Knockout of l-histidine decarboxylase prevents cholangiocyte damage and hepatic fibrosis in mice subjected to high-fat diet feeding via disrupted histamine/leptin signaling. Am J Pathol. 2018;188(3):600–15.
32. Guo M. Cellular senescence and liver disease: Mechanisms and therapeutic strategies. Biomed Pharmacother. 2017; 96:1527–37.
33. Blagosklonny MV. Geroconversion: Irreversible step to cellular senescence. Cell Cycle 2014;13(23):3628–35.
34. Ferreira-Gonzalez S, Lu WY, Raven A, Dwyer B, Man TY, O'Duibhir E, Lewis PJS, Campana L, Kendall TJ, Bird TG, et al. Paracrine cellular senescence exacerbates biliary injury and impairs regeneration. Nat Commun. 2018;9(1):1020.
35. Alpini G, Glaser SS, Ueno Y, Pham L, Podila PV, Caligiuri A, LeSage G, LaRusso NF. Heterogeneity of the proliferative capacity of rat cholangiocytes after bile duct ligation. Am J Physiol. 1998;274(4):G767–75.
36. LeSage G, Glaser S, Marucci L, Benedetti A, Phinizy JL, Rodgers R, Caligiuri A, Papa E, Tretjak Z, Jezequel AM, et al. Acute carbon tetrachloride feeding induces damage of large but not small cholangiocytes from BDL rat liver. Am J Physiol Gastrointest Liver Physiol. 1999;276(5):G1289–301.
37. Mancinelli R, Franchitto A, Gaudio E, Onori P, Glaser S, Francis H, Venter J, Demorrow S, Carpino G, Kopriva S and others. After damage of large bile ducts by gamma-aminobutyric acid, small ducts replenish the biliary tree by amplification of calcium-dependent signaling and de novo acquisition of large cholangiocyte phenotypes. Am J Pathol. 2010;176(4):1790–800.
38. Lunz JG, 3rd, Contrucci S, Ruppert K, Murase N, Fung JJ, Starzl TE, Demetris AJ. Replicative senescence of biliary epithelial cells precedes bile duct loss in chronic liver allograft rejection: increased expression of p21(WAF1/Cip1) as a disease marker and the influence of immunosuppressive drugs. Am J Pathol. 2001;158(4):1379–90.
39. Que KT, Zhou Y, You Y, Zhang Z, Zhao XP, Gong JP, Liu ZJ. MicroRNA-31-5p regulates chemosensitivity by preventing the nuclear location of PARP1 in hepatocellular carcinoma. J Exp Clin Cancer Res. 2018;37(1):268.
40. Li R, Dong J, Bu XQ, Huang Y, Yang JY, Dong X, Liu J. Interleukin-6 promotes the migration and cellular senescence and inhibits apoptosis of human intrahepatic biliary epithelial cells. J Cell Biochem. 2018;119(2):2135–43.
41. Sasaki M, Miyakoshi M, Sato Y, Nakanuma Y. Chemokine–chemokine receptor CCL2–CCR2 and CX3CL1–CX3CR1 axis may play a role in the aggravated inflammation in primary biliary cirrhosis. Dig Dis Sci. 2014;59(2):358–64.
42. Sasaki M, Miyakoshi M, Sato Y, Nakanuma Y. Modulation of the microenvironment by senescent biliary epithelial cells may be involved in the pathogenesis of primary biliary cirrhosis. J Hepatol. 2010;53(2):318–25.
43. Vollmar B, Pradarutti S, Nickels RM, Menger MD. Age-associated loss of immunomodulatory protection by granulocyte-colony stimulating factor in endotoxic rats. Shock 2002;18(4):348–54.
44. Bertolani C, Sancho-Bru P, Failli P, Bataller R, Aleffi S, DeFranco R, Mazzinghi B, Romagnani P, Milani S, Gines P, et al. Resistin as an intrahepatic cytokine: Overexpression during chronic injury and induction of proinflammatory actions in hepatic stellate cells. Am J Pathol. 2006;169(6):2042–53.
45. Sato-Matsubara M, Matsubara T, Daikoku A, Okina Y, Longato L, Rombouts K, Thuy LTT, Adachi J, Tomonaga T, Ikeda K, et al. Fibroblast growth factor 2 (FGF2) regulates cytoglobin expression and activation of human hepatic stellate cells via JNK signaling. J Biol Chem. 2017;292(46):18961–72.
46. Xu H, Liu L, Cong M, Liu T, Sun S, Ma H, You H, Jia J, Wang P. EGF neutralization antibodies attenuate liver fibrosis by inhibiting myofibroblast proliferation in bile duct ligation mice. Histochem Cell Biol 2020;154:107–16.
47. Niu B, He K, Li P, Gong J, Zhu X, Ye S, Ou Z, Ren G. SIRT1 upregulation protects against liver injury induced by a HFD through inhibiting CD36 and the NFkappaB pathway in mouse kupffer cells. Mol Med Rep. 2018;18(2):1609–15.
48. Childs BG, Baker DJ, Kirkland JL, Campisi J, van Deursen JM. Senescence and apoptosis: Dueling or complementary cell fates? EMBO Rep. 2014;15(11):1139–53.